Modulated waves and pattern formation in coupled discrete nonlinear *LC* transmission lines

Fabien II Ndzana,[1,*] Alidou Mohamadou,[1,2,3,†] Timoléon C. Kofané,[1,‡] and Lars Q. English[3]
[1]*Laboratory of Mechanics, Department of Physics, Faculty of Science, University of Yaounde I, P.O. Box 812, Yaounde, Cameroon*
[2]*Condensed Matter Laboratory, Department of Physics, Faculty of Science, University of Douala, P.O. Box 24157, Douala, Cameroon*
[3]*Department of Physics and Astronomy, Dickinson College, Carlisle, Pennsylvania 17013, USA*
(Received 9 January 2008; revised manuscript received 1 May 2008; published 29 July 2008)

The conditions for the propagation of modulated waves on a system of two coupled discrete nonlinear *LC* transmission lines with negative nonlinear resistance are examined, each line of the network containing a finite number of cells. Our theoretical analysis shows that the telegrapher equations of the electrical transmission line can be reduced to a set of two coupled discrete complex Ginzburg-Landau equations. Using the standard linear stability analysis, we derive the expression for the growth rate of instability as a function of the wave numbers and system parameters, then obtain regions of modulational instability. Using numerical simulations, we examine the long-time dynamics of modulated waves in the line. This leads to the generation of nonlinear modulated waves which have the shape of a soliton for the fast and low modes. The effects of dissipative elements on the propagation are also shown. The analytical results are corroborated by numerical simulations.

DOI: 10.1103/PhysRevE.78.016606 PACS number(s): 05.45.Yv, 42.65.Tg, 84.40.Az, 42.25.Bs

I. INTRODUCTION

Wave propagation in nonlinear periodic lattices is associated with a lot of exciting phenomena that have no counterpart whatsoever in bulk media. Perhaps, the most intriguing entities that can exist in such systems are discrete self-localized states—better known as discrete solitons [1]. Over the years, discrete solitons have been a topic of intense investigation in several branches of science such as atomic chains [2], with on-site cubic nonlinearities, molecular crystals [3], biophysical systems [4], Bose-Einstein condensates [5], and electrical lattices [6,7]. In fact, nonlinear transmission lines (NLTLs) are very convenient tools to study wave propagation in nonlinear dispersive media [8]. In particular, they provide a useful way to check how the nonlinear excitations behave inside the nonlinear medium and to model the exotic properties of new systems [9]. These are the reasons why, since the pioneering works by Hirota and Suzuki [10] and Nagashima and Amagishi [11] on a single electrical lines simulating the Toda lattice [12], a growing interest has been devoted to the use of NLTLs. As we said above, NLTLs have the capacity to support solitons such as excitations (kinks, pulses, envelope, bright, dark solitons, etc.) [6,13]. Solitons are localized pulses that arise in many physical contexts through a balance of nonlinearity and dispersion. Since the 1970s, various investigators have discovered the existence of solitons in NLTLs, through both mathematical models and physical experiments. An envelope soliton can be viewed as a results of an instability that leads to a self-induced modulation of the steady state produced by the interaction between nonlinear and dispersive effects. It has been shown that the system of equations governing the physics of the NLTL can be reduced to the Korteweg–de Vries (KdV) equation, the continuous and discrete nonlinear Schrödinger (NLS and DNLS) equations [6,14], the continuous and discrete complex Ginzburg-Landau (CGL and DCGL) equations [7,15], and the continuous coupled nonlinear Schrödinger (CNLS) equation [16]. All these equations admit modulational instability (MI) and the formation of envelope solitons, which have been observed experimentally [6–16].

There are only a few works that we know of which report the study of solitons in the coupled NLTL. Kakutamni and Yamasaki [17] have investigated theoretically and experimentally the KdV solitons on a coupled *LC* transmission line consisting of two nonlinear *LC* ladder lines connected by identical intermediary capacitors and have shown that the network admits two different modes (a fast mode and a slow mode) in each direction of wave propagation. Next, an extension of these studies to envelope solitons was made by Essimbi *et al.* [18]. Quite recently, Yemele and Kofane [18] as well as Kengne *et al.* [16] modeled this coupled line by a set of CNLS equations. The soliton propagation and interaction on two-dimensional nonlinear transmission lines have also been studied (see [19] and references therein). However, experiments and analytical studies on the basic coupled NLTL show that whenever the network is excited by an electrical wave, two modes of propagation (slow and fast modes) are generated in each line and enter unavoidably into play with the wave-coupling behavior, causing qualitatively different phenomena compared with the ordinary process of MI, such as the annihilation of both modes. Periodic structures have an even richer variety of properties when they are dissipative—i.e., have gained and lost in the system. In particular, discrete analogs of the CGL equation have drawn attention in the field of pattern formation in nonlinear coupled oscillators [20].

The most standard mechanism through which bright solitons and solitary wave structures appears is through activation of the MI of plane waves. In this case, the continuous-wave solution of the NLS equation or CGL equation

*ndzanafabienii@yahoo.com
†mohdoufr@yahoo.fr
‡tckofane@yahoo.com

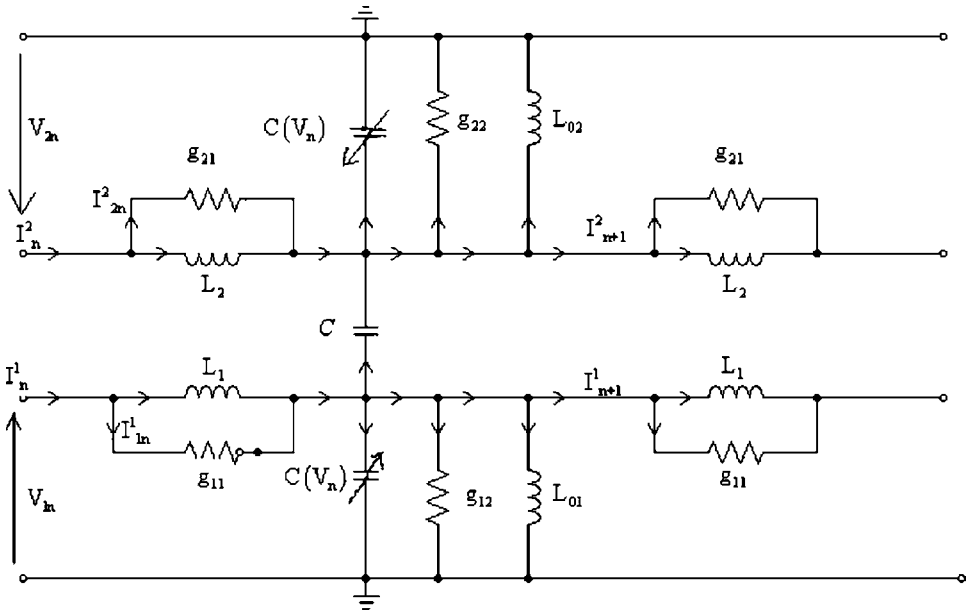

FIG. 1. Schematic representation of the electrical line.

becomes unstable toward the generation of a chain of bright soliton. Therefore, it is useful to model the coupled NLTLs by a system of two DCGL equations and, hence, present carefully analytical and numerical investigations concerning the nonlinear modulated waves, the possible free propagation of envelope solitons on the two coupled NLTLs.

The structure of the paper is as follows. In Sec. II we present the basic characteristics of the coupled NLTLs under consideration. Then, we will focus on deriving the coupled discrete complex Ginzburg-Landau (CDCGL) equation. Based on the obtained CDCGL equation, we determined the frequency domain where the network allows the propagation of envelope solitons in Sec. III. Numerical investigations are performed in Sec. IV in order to verify the validity of theoretical predictions—namely, the MI phenomenon and the propagation of solitonic waves. Finally, concluding remarks are presented to Sec. V.

II. BASIC COUPLED NONLINEAR DISCRETE *LC* TRANSMISSION LINES

The model used in this work consists of a nonlinear network with two coupled nonlinear transmission lines. Each line contains a finite number of cells which consist of two elements: a linear inductor of inductance L_j in the series branch and a nonlinear capacitor of capacitance C_j in the shunt branch. This capacitor consists of a reverse-biased diode with a differential capacitance function of the voltage V_{jn}

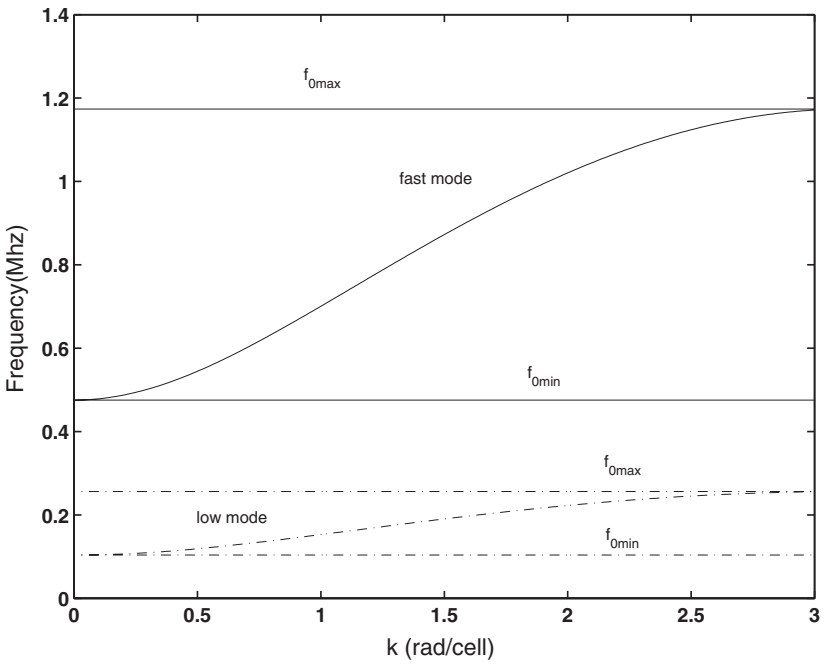

FIG. 2. Linear dispersion curves for the two modes as a function of the wave number k for $0 \leq k \leq \pi$.

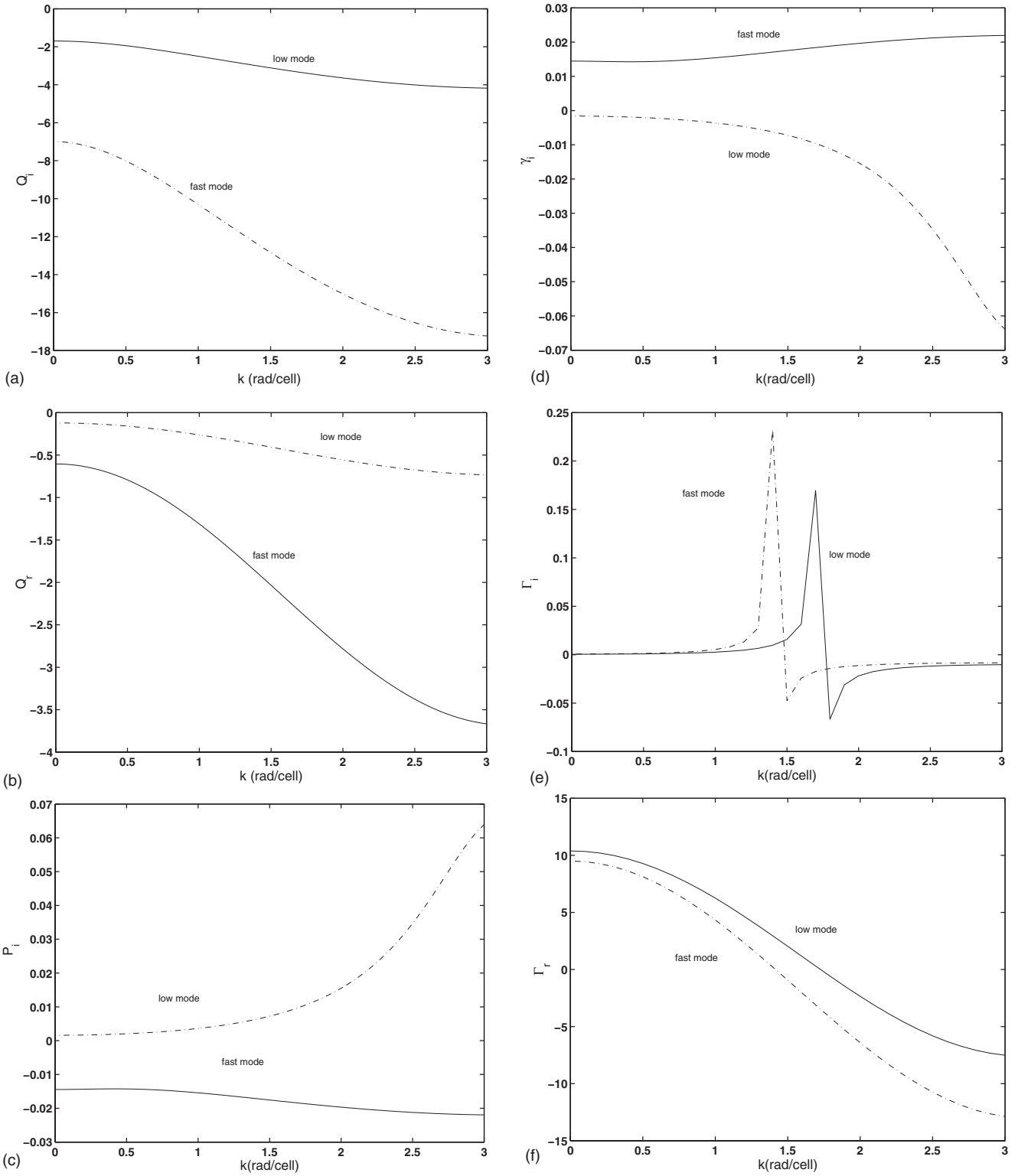

FIG. 3. Coefficients of the DCGL equation as a function of the wave number k for $0 \leq k \leq \pi$. (a) Imaginary part of the nonlinearity coefficient. (b) Real part of the nonlinearity coefficient. (c) Imaginary part of the dispersion coefficient. (d) Imaginary part of the coupled coefficient. (e) Real part of the coupled coefficient

across the jnth capacitor. In order to take into account the dissipation of the network, the conductances g_{1j} and g_{2j} are connected in parallel with L_j and L_{0j}, respectively. The conductance g_{1j} describes the dissipation in the inductor L_j, while g_{2j} accounts for the dissipation of the inductor L_{0j} in addition to the loss of the nonlinear capacitance C_j; the subscript j designates the line number and can take the values 1 and 2. The two lines are connected by an intermediary linear capacitor C, as shown in Fig. 1. The following values of the parameters are used for our study: $L_1 = L_2 = 220$ μH and

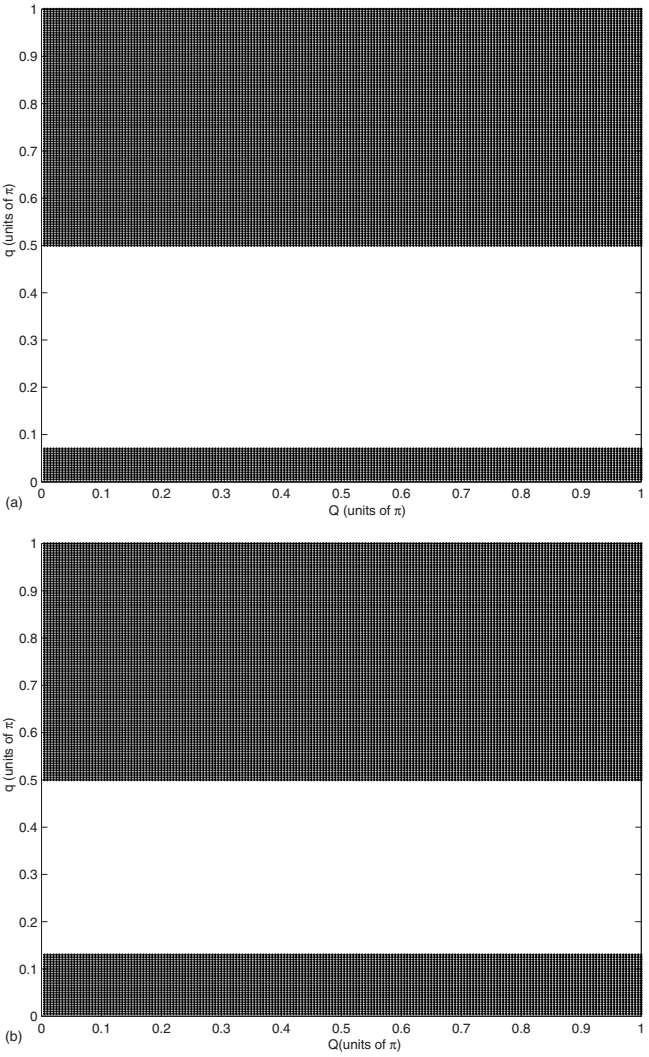

FIG. 4. Domain of modulational instability on the (Q,q) plane. (a) Fast mode. (b) Slow mode.

$L_{01}=L_{02}=280$ μH [6,14,15]. The nonlinearity is introduced in the line by a varicap diode for which the capacitance varies with the applied voltage. Denoting by $Q_{nj}(t)$ the nonlinear electrical charge of the jnth cell and by $V_{jn}(t)$ the corresponding voltage, we assume that the charge has a voltage dependence similar to the one of an electrical Toda lattice [7,12]:

$$Q_{nj}(t) = C_{0j}A \ln\left(1 + \frac{V_{jn}}{A}\right), \tag{1}$$

where A and C_{0j} are constants. Negative nonlinear resistances are defined by their nonlinear current-voltage characteristics. They are made of operational amplifiers, transistors, or multipliers. They were introduced recently in nonlinear transmission lines for signal-processing applications, particularly in noise removal on coherent information weakly varying in space [21] and on image and wave amplification [22,23]. The corresponding conductance is given by

$$g_{2j} = \alpha - \beta V_{jn}. \tag{2}$$

We focus now on the propagation of nonlinear waves through the lattice. From Kirchhoff's laws it is easy to show that the propagation of waves in the network is governed by the following equation:

$$\begin{aligned}
&(A + V_{jn})\frac{d^2V_{jn}}{dt^2} - \left(\frac{dV_{jn}}{dt}\right)^2 \\
&\quad = \frac{\mu_{0j}^2}{A}(A + V_{jn})^2(V_{jn-1} - 2V_{jn} + V_{jn+1}) \\
&\qquad + 2\sigma_1\frac{\mu_{0j}}{A}(A + V_{jn})^2\left(\frac{d(V_{jn-1} - 2V_{jn} + V_{jn+1})}{dt}\right) \\
&\qquad - \frac{\omega_{0j}^2}{A}(A + V_{jn})^2V_{jn} - 2\sigma_2\frac{\mu_{0j}}{A}(A + V_{jn})^2\frac{dV_{jn}}{dt} \\
&\qquad + \frac{\beta}{AC_{0j}}(A + V_{jn})^2\frac{dV_{jn}^2}{dt} \\
&\qquad + \frac{\lambda_j}{A}(A + V_{jn})^2\left[\frac{d^2V_{3-jn}}{dt^2} - \frac{d^2V_{jn}}{dt^2}\right].
\end{aligned} \tag{3}$$

For the sake of convenience, the dimensionless σ_1, σ_2, and λ_j are introduced, they are related to conductance g_1, g_2, and C as $g_1/C_{01}=2\mu_0\sigma_1$, $g_2/C_{01}=2\mu_0\sigma_2$, and $C/C_{0j}=\lambda_j$.

The linear properties of the network can be studied by assuming a sinusoidal wave of the form

$$V_{jn}(t) = V_j \exp[i(kn - \omega t)] + \text{c.c.}, \tag{4}$$

where k and ω are the wave number and the angular frequency, respectively, and "c.c." stands for the complex conjugate. The dispersion relation of the line is obtained after solving the following system:

$$\begin{pmatrix} d_{11} & d_{12} \\ d_{21} & d_{22} \end{pmatrix}\begin{pmatrix} V_1 \\ V_2 \end{pmatrix} = \begin{pmatrix} 0 \\ 0 \end{pmatrix}, \tag{5}$$

where the coefficients of the matrices are given in Appendix A. Equation (5) leads to the following dispersion expression:

$$\omega_l^2 = \frac{-b + (-1)^l\sqrt{\Delta}}{2a}, \tag{6}$$

where the coefficients a, b, c, and Δ are defined in Appendix A. Equation (6) explains that there are two elementary wave (modes) which coexist on each line at the same frequency ω, but with different wave numbers. The mode corresponding to $l=2$ has a higher group velocity compared with the group velocity of the mode $l=1$: it is the fast mode. Accordingly, the mode $l=1$ is called the slow mode. Figure 2 shows, for different situations, the linear dispersion curves of these two modes of propagation. When the two coupled lines have identical linear characteristic parameters—i.e., $\omega_{01}=\omega_{02}=\omega_0$, $\mu_0=\mu_{01}=\mu_{02}$, and $\lambda_2=\lambda_1=\lambda$—the fast mode reduces to the standard mode of propagation of an isolated single line with the characteristic frequency

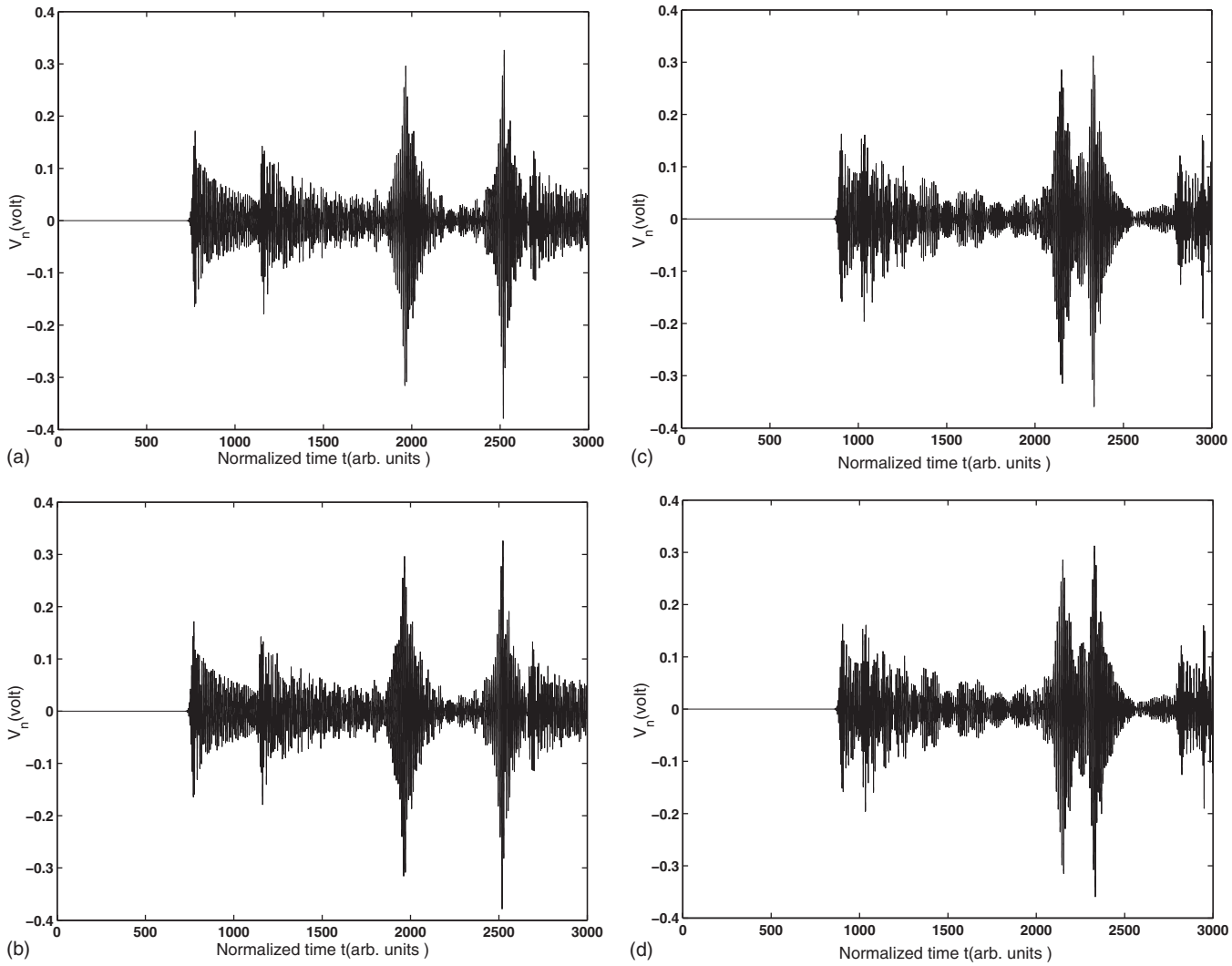

FIG. 5. Propagation of waves through the network for the slow mode in the absence of dissipative elements ($\sigma_1=0,\sigma_2=0$). (a) For line 1, cell 800. (b) For line 2, cell 800. (c) For line 1, cell 1000. (d) For line 2, cell 1000.

$$\omega_2^2 = \omega_0^2 + 4\mu_0^2 \sin^2\left(\frac{k}{2}\right), \tag{7}$$

while the characteristic frequency of the slow mode reduces to

$$\omega_1^2 = \frac{\omega_0^2 + 4\mu_0^2 \sin^2(k/2)}{1+2\lambda}. \tag{8}$$

The amplitudes of the signal voltage propagating along the two coupled lines are linearly dependent and satisfy the relation $V_2^l = \eta V_1^l$, where $l=1,2$ and

$$\eta^l = 1 + \frac{1}{\lambda}\left(1 - \frac{\omega_0^2 + 4\mu_0^2 \sin^2(k/2)}{\omega_1^2}\right). \tag{9}$$

The superscript l stands for the mode propagation. Hereafter, we shall use this notation where the case $l=1$ stands for the slow mode and the case $l=2$ corresponds to the fast mode. To describe modulated waves in the network, we consider waves with slow temporal variations of the envelope. We look for a solution of Eq. (3) in the form

$$V_{jn} = \varepsilon \psi_{jn}(T) e^{(-i\omega t)} + \varepsilon \psi_{jn}^*(T) e^{(i\omega t)}, \tag{10}$$

where ε is a small parameter and $T=\varepsilon^2 t$. Inserting this relation into Eq. (3) and collecting solutions of order $(\varepsilon^n, \exp(-i\omega t))$, the following relation has been derived at order $(\varepsilon, \exp(-i\omega t))$:

$$\psi_{jn}[\omega_{0j}^2 + 2\mu_{0j}^2 - (1+\lambda_j)\omega^2] = \mu_{0j}^2(\psi_{jn-1} + \psi_{jn+1}) - \lambda_j \omega^2 \psi_{3-jn}. \tag{11}$$

At order $(\varepsilon^2, 1)$ we have

$$\mu_{0j}^2(\psi_{jn-1}^* + \psi_{jn+1}^* - 2\psi_{jn}^*)\psi_{jn}^2 - \lambda_j \omega^2(\psi_{3-jn}^* \psi_{jn}^2 + \psi_{3-jn}|\psi_{jn}|^2) = 2[\omega_{0j}^2 - (1+\lambda_j)\ \omega^2)]|\psi_{jn}|^2 \psi_{jn} - \mu_{0j}^2(\psi_{jn-1} + \psi_{jn+1} - 2\psi_{jn}) \times |\psi_{jn}|^2. \tag{12}$$

The solution of order $(\varepsilon^3, \exp(-i\omega t))$ is given by the following equation:

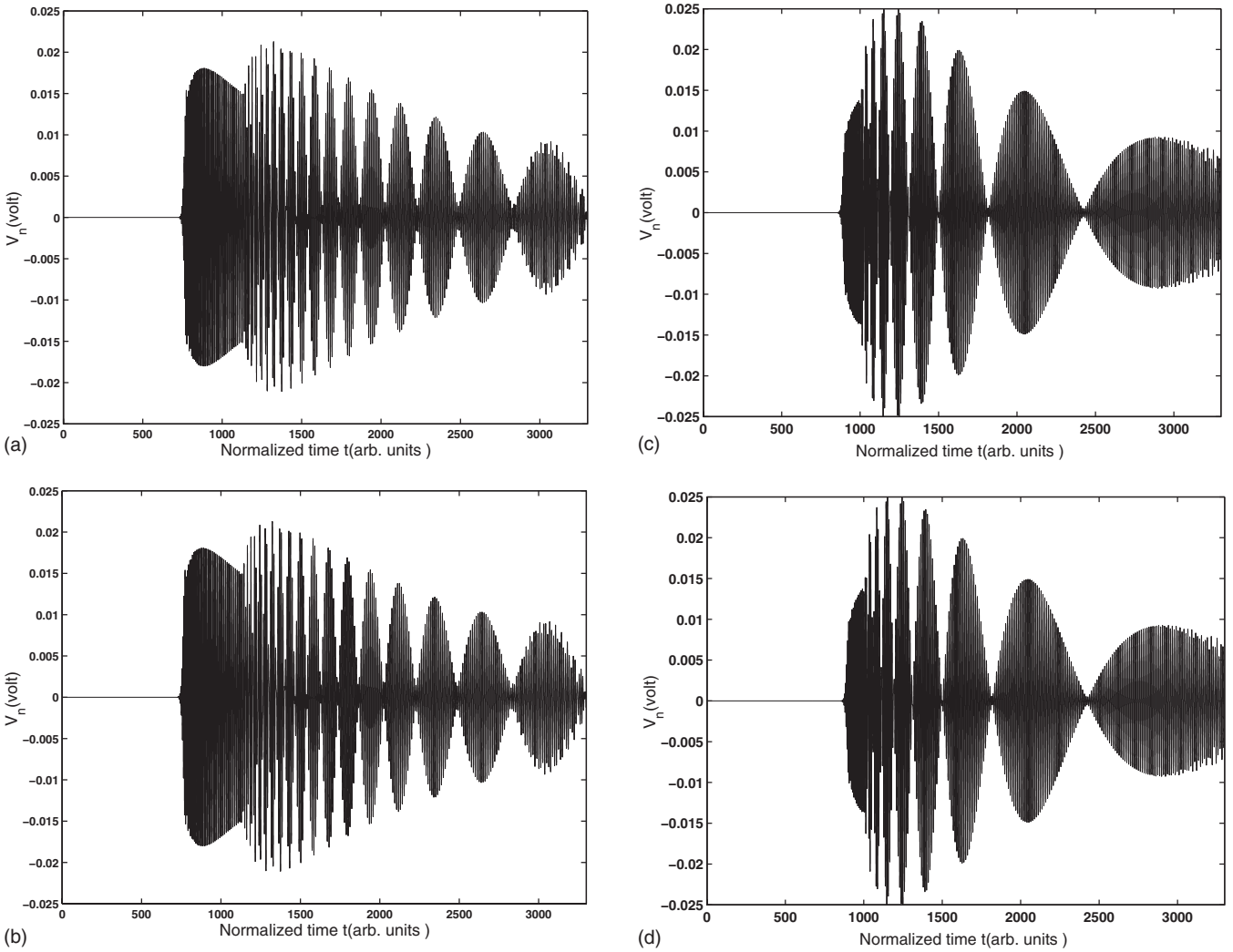

FIG. 6. Propagation of waves through the network for the slow mode in the presence of dissipative elements ($\sigma_1=0.00461, \sigma_2=0.0$). (a) For line 1, cell 800. (b) For line 2, cell 800. (c) For line 1, cell 1000. (d) For line 2, cell 1000.

$$
\begin{aligned}
&-2i\omega\psi_{jnT}+\frac{2i\omega\lambda_j}{1+\lambda_j}\psi_{3-jnT}+\left[\frac{3\omega^2}{A^2(1+\lambda_j)}+\frac{4i\beta_{0j}\omega}{(1+\lambda_j)A}\right]\\
&\quad\times|\psi_{jn}|^2\psi_{jn}+\frac{2i\mu_{0j}\omega}{(1+\lambda_j)}\\
&\quad\times\left[\frac{\sigma_1(\omega_{0j}^2+2\mu_{0j}^2-(1+\lambda_j)\omega^2)-\mu_{0j}^2(\sigma_2+2\sigma_1)}{\omega_{0j}^2+2\mu_{0j}^2-(1+\lambda_j)\omega^2}\right]\\
&\quad\times(\psi_{jn+1}+\psi_{jn-1})\\
&\quad=\left(\frac{2i\lambda_j\mu_{0j}\omega^3(\sigma_2+2\sigma_1)}{(1+\lambda_j)(\omega_{0j}^2+2\mu_{0j}^2-(1+\lambda_j)\omega^2)}\right)\psi_{3-jn}. \qquad (13)
\end{aligned}
$$

Let us set $\psi_{jn}=\phi_{jn}\exp[\frac{\omega_{0j}^2+2\mu_{0j}^2-(1+\lambda_j)\omega^2}{\mu_{0j}^2}]\tau$ and $\tau=\frac{\mu_{0j}^2}{2\omega}T$. The previous equation hence yields

$$
\begin{aligned}
&i\phi_{jn\tau}+i\alpha_j\phi_{3-jn\tau}+P_j(\phi_{jn-1}-2\phi_{jn}+\phi_{jn+1})+Q_j|\phi_{jn}|^2\phi_{jn}\\
&\quad=\gamma_j\phi_{jn}+\Gamma_{3-j}\phi_{3-jn}, \qquad (14)
\end{aligned}
$$

where the coefficients $P_j=(P_{jr}+iP_{ji})$, $Q_j=(Q_{jr}+iQ_{ji})$, $\gamma_j=(\gamma_{jr}+i\gamma_{ji})$, and $\Gamma_j=(\Gamma_{jr}+i\Gamma_{ji})$ are expressed in Appendix A and depend on the wave number k (Fig. 3 presents the shape of these coefficients). This equation has a long history as a generic amplitude equation derived asymptotically near the onset of instabilities in fluid dynamical systems. The case with complex coefficients was put forth in a general setting by Newell and Whitehead [24] and DiPrima *et al.* [26] and was applied by Stewartson and Stuart [25] to plane Poiseuille flow. Equation (14), which describes the evolution of a complex value $\phi_{jn}=\phi_{jn}(n,\tau)$, is the coupled discrete complex Ginzburg-Landau equation. Accordingly, Eq. (14) constitutes two sets of two coupled DCGL equations corresponding to the two different lines of the network. The study of physical and mathematical aspects of coupled nonlinear equations is of considerable interest as these equations arise in diverse areas of science such as nonlinear optics, optical communication, biophysics, Bose-Einstein condensates, plasma physics, and electrical transmission lines. The single DCGL equation is known to play a ubiquitous role in science. These DCGL lattices are quite often known to describe a number of

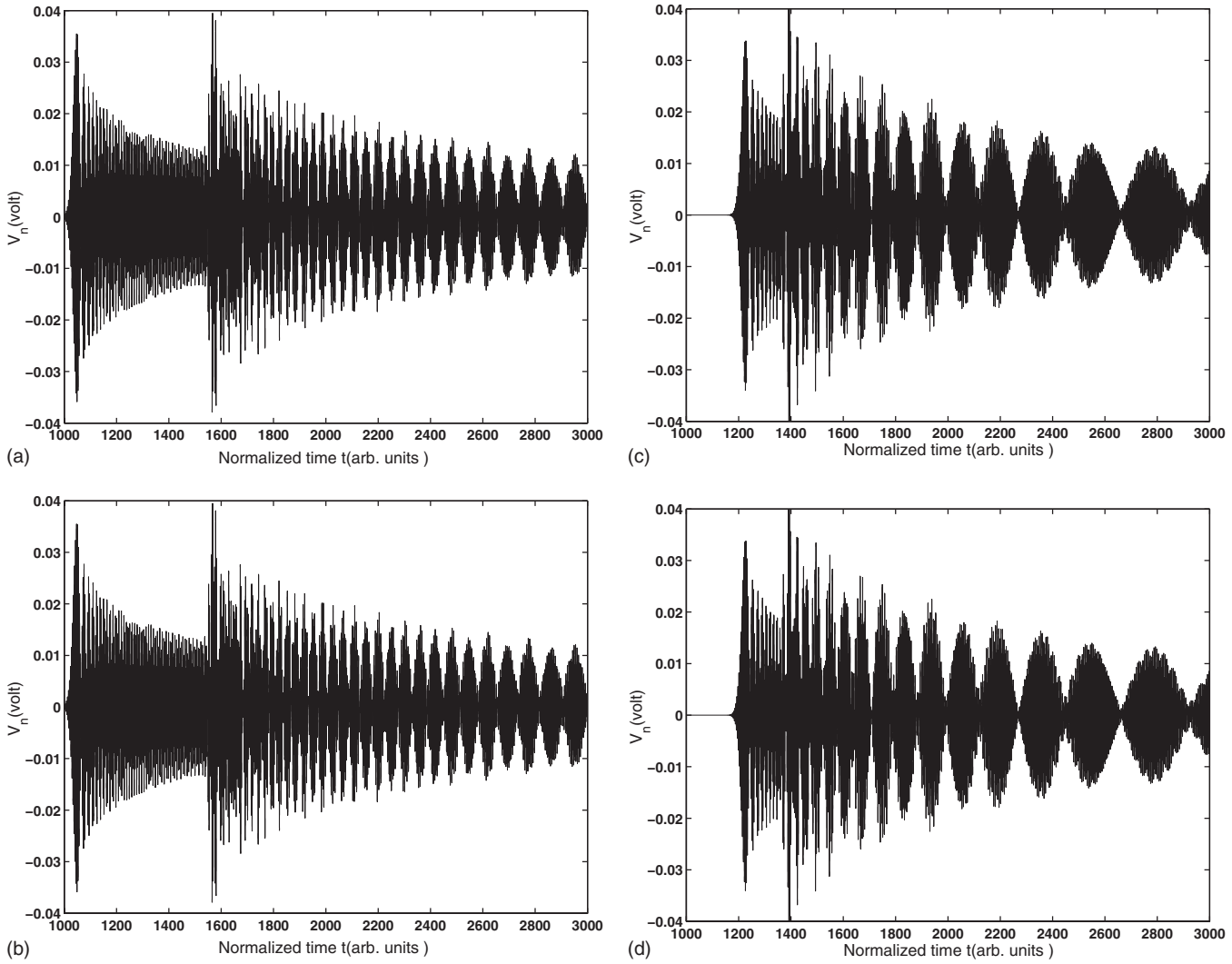

FIG. 7. Propagation of waves through the network for the fast mode in the absence of dissipative elements ($\sigma_1=0, \sigma_2=0$). (a) For line 1, cell 600. (b) For line 2, cell 600. (c) For line 1, cell 800. (d) For line 2, cell 800.

physical systems such as Taylor and frustrated vortices in hydrodynamics [27] and semiconductor laser arrays in optics [28] as well as pulse propagation. Recently, Porsezian *et al.* [29] investigated the MI of symmetric and asymmetric continuous solutions in a model of a laser based on a dual-core nonlinear optical fiber based on the continuous cubic-quintic CGL equation.

When the coefficients P_{ji}, Q_{ji}, and γ_{ji} are equal to zero, Eq. (14) is reduced to the CNLS equation. The CNLS equation has been used to describe motions and interactions of more than one wave envelope in cases in which more than first-order parameters are needed to specify the system. It can be used to describe the interactions of solitons in a baroclinic atmosphere [30,29], the suppression of forward and backward propagating modulated waves in a single electrical transmission line [31], and the evolution of two linear polarization components in nonlinear birefringent optical fibers [32], to cite just a few.

As we just saw, interest in the dynamic of discrete systems comes from the diversity of their numerous applications in physical and biological sciences. Through the present study, we see that the small-amplitude pulses on systems of coupled NLETL via constant capacitors are described by a set of CDCGL equations. This system possesses a traveling-wave solution that can be unstable under linear perturbations.

III. MODULATIONAL INSTABILITY STUDIES OF THE CDCGL EQUATION

Modulational instability has time-honored history in nonlinear wave equations. Over the years, MI has been observed in various physical settings, including hydrodynamics, plasma physics, nonlinear optics, and quite recently in Bose-Einstein condensates. In this section, we will produce characteristics of the MI in the form of a typical dependence of the instability growth rate on the wave numbers and system parameters. Let us recall explicitly the CDCGL equations

$$i\phi_{1n\tau} + i\alpha_1\phi_{2n\tau} + (P_{1r} + iP_{1i})(\phi_{1n-1} - 2\phi_{1n} + \phi_{1n+1}) + (Q_{1r} + iQ_{1i})|\phi_{1n}|^2\phi_{1n} = (\gamma_{1r} + i\gamma_{1i})\phi_{1n} + (\Gamma_{1r} + i\Gamma_{1i})\phi_{2n},$$

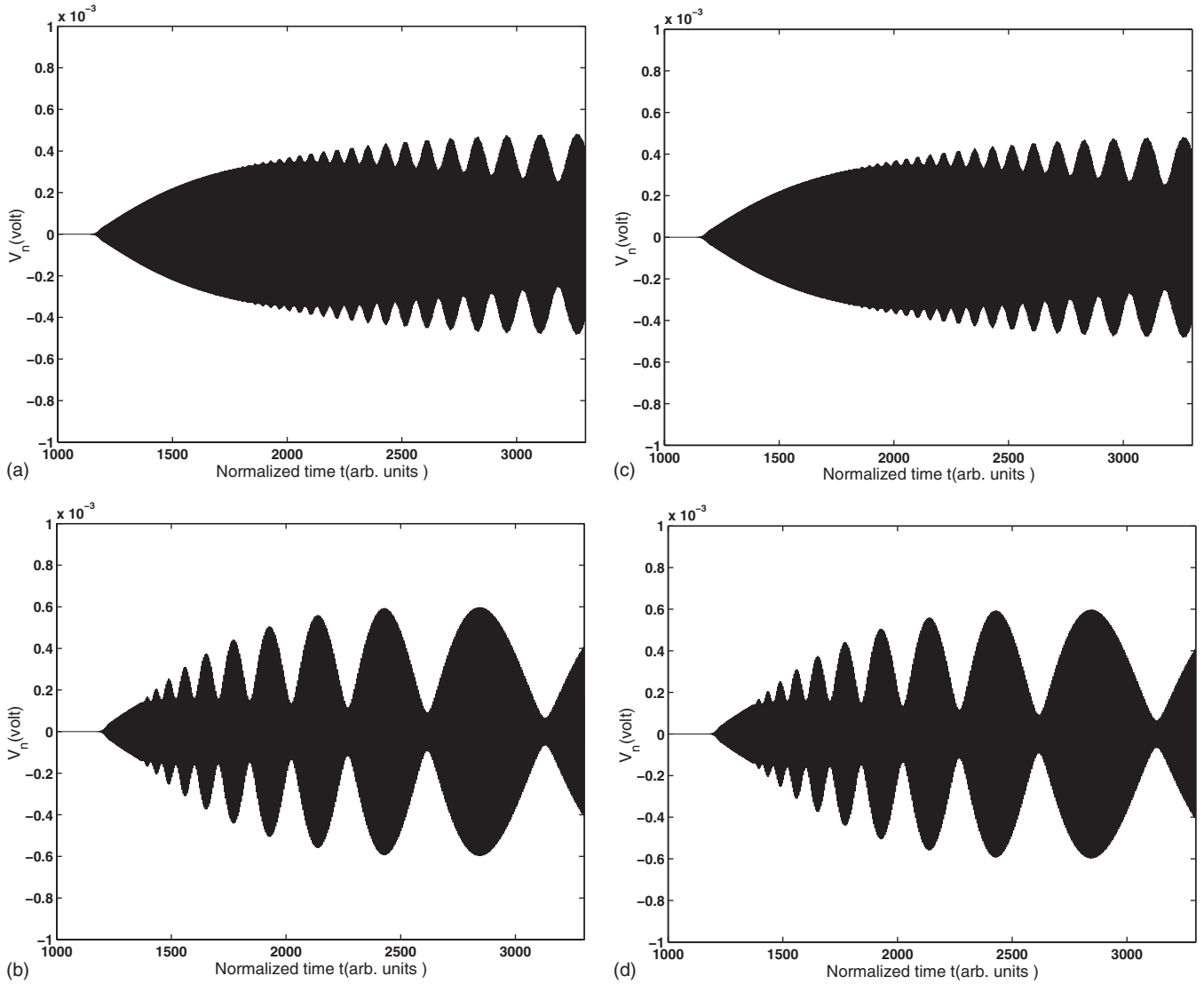

FIG. 8. Propagation of waves through the network for the fast mode in the presence of dissipative elements ($\sigma_1=0.00461, \sigma_2=0.0$). (a) For line 1, cell 600. (b) For line 2, cell 600. (c) For line 1, cell 800. (d) For line 2, cell 800.

$$i\phi_{2n\tau} + i\alpha_2\phi_{1n\tau} + (P_{2r} + iP_{2i})(\phi_{2n-1} - 2\phi_{2n} + \phi_{2n+1}) + (Q_{2r} + iQ_{2i})|\phi_{2n}|^2\phi_{2n} = (\gamma_{2r} + i\gamma_{2i})\phi_{2n} + (\Gamma_{2r} + i\Gamma_{2i})\phi_{1n}. \quad (15)$$

We look for plane-wave solutions in the form

$$\phi_{jn}(\tau) = \Lambda_j e^{[i(q_j n - \Omega_j \tau)]}, \quad j = 1,2. \quad (16)$$

The linear coupling imposes the restrictions $q_1=q_2=q$ and $\Omega_1=\Omega_2=\Omega_0$. Inserting Eq. (16) into Eq. (15), we obtain the following expression describing implicitly the characteristics of the continuous-wave solution: the real parts of this relation,

$$\Omega_0(\Lambda_1 + \alpha_1\Lambda_2) = -2P_{1r}\cos(q)\Lambda_1 - Q_{1r}|\Lambda_1|^2\Lambda_1 + \Gamma_1\Lambda_2,$$

$$\Omega_0(\alpha_2\Lambda_1 + \Lambda_2) = -2P_{2r}\cos(q)\Lambda_2 - Q_{2r}|\Lambda_2|^2\Lambda_2 + \Gamma_2\Lambda_1, \quad (17)$$

and the imaginary parts of this relation,

$$2P_{1i}\Lambda_1\cos(q) + Q_{1i}|\Lambda_1|^2\Lambda_1 = \Gamma_{1i}\Lambda_2,$$

$$2P_{2i}\Lambda_2\cos(q) + Q_{2i}|\Lambda_2|^2\Lambda_2 = \Gamma_{2i}\Lambda_1. \quad (18)$$

Let us now consider a small perturbation around the stationary plane waves:

$$\phi_{jn}(\tau) = [\Lambda_j + B_{jn}(\tau)]e^{[i(qn - \Omega_0\tau)]}, \quad (19)$$

where B_{jn} is a complex function denoting the small perturbation of the slowly varying modulated complex amplitude. Substituting this relation into Eq. (15), one obtains a linearized equation for the perturbations B_{jn}:

$$iB_{1n\tau} + P_1[(B_{1n-1} - 2B_{1n} + B_{1n+1})\cos(q) + i(B_{1n+1} - B_{1n-1})\sin(q)] + [\Gamma_1 - \alpha_1\Omega_0]\frac{\Lambda_2}{\Lambda_1}B_{1n} + Q_1|\Lambda_1|^2(B_{1n} + B_{1n}^*) = -i\alpha_1 B_{2n\tau} + (\Gamma_1 - \alpha_1\Omega_0)B_{2n},$$

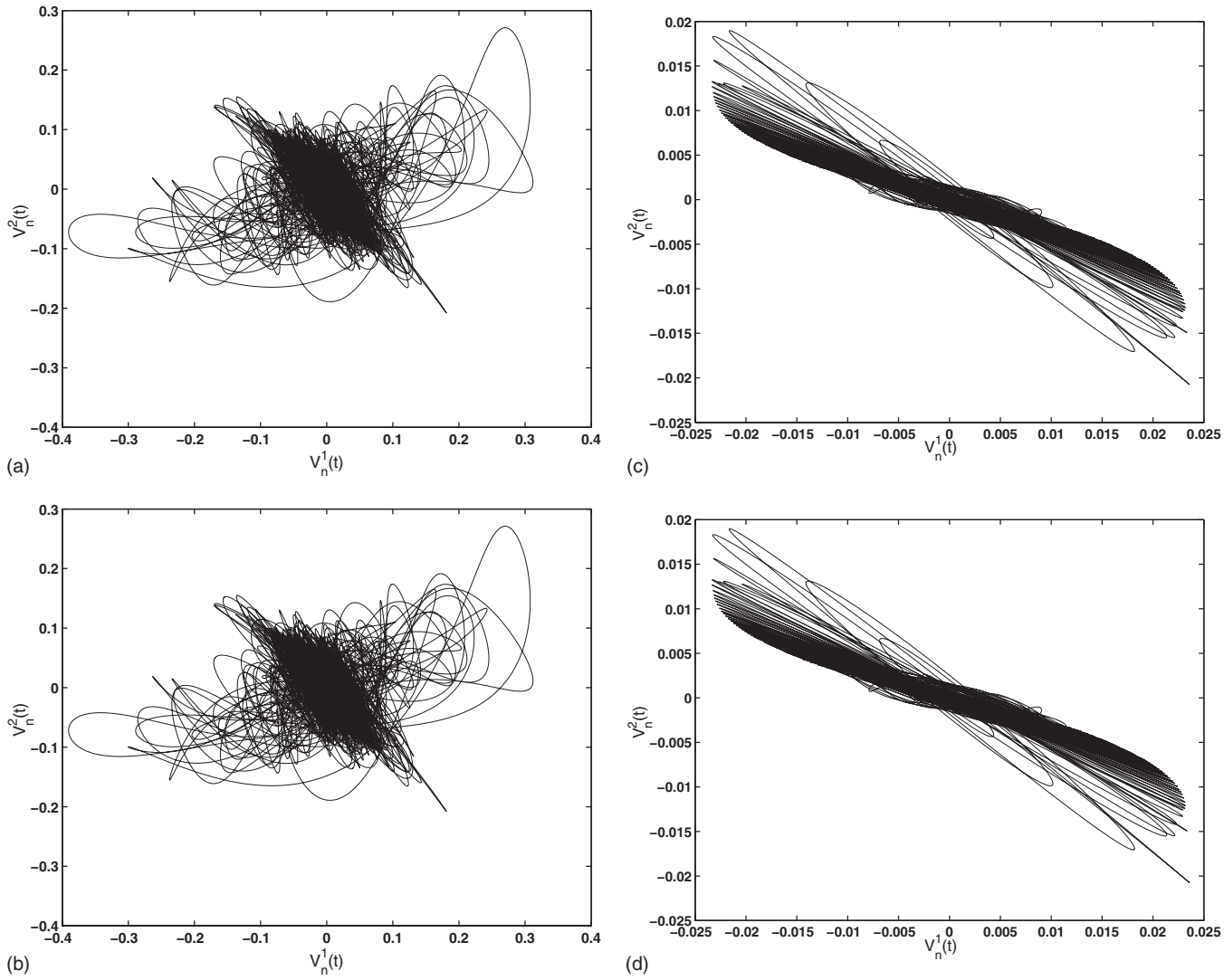

FIG. 9. Phase portrait of the low mode at cell 1000. (a) In the absence of dissipation, line 1. (b) Line 2. (c) In the presence of dissipation, cell line 2. (d) Line 2.

$$
\begin{aligned}
&iB_{2n\tau} + P_2[(B_{2n-1} - 2B_{2n} + B_{2n+1})\cos(q) \\
&\quad + i(B_{2n+1} - B_{2n-1})\sin(q)] + [\Gamma_2 - \alpha_2\Omega_0]\frac{\Lambda_1}{\Lambda_2}B_{2n} \\
&\quad + Q_2|\Lambda_2|^2(B_{2n} + B_{2n}^*) \\
&\quad = -i\alpha_2 B_{1n\tau} + (\Gamma_2 - \alpha_2\Omega_0)B_{1n}. \qquad (20)
\end{aligned}
$$

Furthermore, we assume a general solution of the above-mentioned system in the form

$$
B_{jn}(\tau) = a_j e^{[i(Qn+\Omega\tau)]} + b_j^* e^{[-i(Qn+\Omega^*\tau)]}, \qquad (21)
$$

where Q and Ω are an arbitrary real wave number of the perturbation and the corresponding propagation frequency, respectively, which is complex in the general case, a_j and b_j being perturbation amplitudes. Hence, substituting this perturbation into Eq. (20), we arrive at a set of linear homogeneous equations for a_j and b_j. This set of homogeneous equations can be written in matrix form as

$$
\mathbf{M} \times (a_1, b_1, a_2, b_2)^T = 0, \qquad (22)
$$

where $\mathbf{M}$ is a 4×4 matrix whose elements h_{pq}, $p,q = 1,2,3,4$, are given in Appendix B. The dispersion relation, which determines Ω as a function of Q, q, and the parameter system, including the MI gain $\sigma \equiv \mathrm{Im}(\Omega)$, is obtained from the condition of the existence of nontrivial solutions of the algebraic linear homogeneous system $\det(\mathbf{M}) = 0$, which amounts to a quartic equation for Ω. This matrix form can be written as

$$\mathbf{M} = \begin{pmatrix} -\Omega + m_1 + im_2 & m_3 + im_4 & -\alpha_1\Omega + m_5 + im_6 & 0 \\ m_3 - im_4 & \Omega + m_1 - im_2 & 0 & \alpha_1\Omega + m_7 - im_6 \\ -\alpha_2\Omega + m_8 + im_9 & 0 & -\Omega + m_{10} + im_{11} & m_{12} + im_{13} \\ 0 & \alpha_2\Omega + m_{14} - im_9 & m_{12} - im_{13} & \Omega + m_{10} - im_{11} \end{pmatrix}. \tag{23}$$

With the frequency in the form $\Omega = \Omega_r + i\sigma$, one can note that $e^{-\sigma\tau}$ enters inside the amplitude of the perturbation. The asymptotic behavior of the perturbation is related to the sign of the constant σ. So an instability may develop in the coupled line if $\mathrm{Im}(\Omega)$ is negative. Thereafter, we solve the condition of the existence of nontrivial solutions using a MATLAB code and we only keep the values of the wave numbers q and Q, which give negative values of the growth rate $\sigma \equiv \mathrm{Im}(\Omega)$ [20,33]. Figure 4 presents regions of MI in the (q,Q) plane for the fast mode [Fig. 4(a)] and slow mode [Fig. 4(b)]. One observes that regions of instability increase slightly in the case of the slow mode.

IV. NUMERICAL RESULTS

According to the analytical calculations presented in Sec. III, the stability of modulated plane waves is fulfilled when the instability growth rate is positive. However, this stability analysis has been obtained through Eq. (14), which is only an approximate description of the initial equation (3). Therefore, the linear stability analysis can only detect the onset of instability, but it does not tell us anything about the behavior of the system when the instability takes places. In order to check the validity of the analytical predictions of MI presented in the previous sections, we have performed numerical simulations on the general equation (3) governing wave propagation in the coupled NLTL. The parameters of the lines are $L_1 = L_2 = 220\ \mu\mathrm{H}$, $L_{01} = L_{02} = 280\ \mu\mathrm{H}$, $C_{01} = C_{02} = 400pF$, $\lambda = 1/2$, $\alpha = 2\mu_0\sigma_2$, and $g_1/C_0 = 2\mu_0\sigma_1$, $\alpha/C_0 = 2\mu_0\sigma_2$ with $\sigma_1 = 0.00461$ and $\sigma_2 = 0$ [6,14,15,18]. The fourth-order Runge-Kutta scheme is used with a normalized integration time step $\Delta t = 5 \times 10^{-3}$. Similarly, the number of cells is chosen so that we do not encounter the wave reflection at the end of the line. At the input of the lines, we apply a slowly modulated signal:

$$V_j(t) = V_{j0}[1 + m_0 \cos(2\pi f_m t)]\cos(2\pi f_p t), \tag{24}$$

where V_{j0} is the amplitude of the unperturbed plane wave (carrier wave), m_0 designates the modulation rate, and f_m is the frequency of modulation. As a specific example, we use the following values for the parameters: $V_{j0} = 1.5$ V, $f_p = 1180$ kHz, $m_0 = 0.01$, and $f_m = 16$ kHz.

Figure 5 shows an example of waves propagating through the network where the corresponding mode of propagation is the slow mode in the absence of dissipation terms ($\sigma_1 = \sigma_2 = 0$). This figure represents the signal voltage at different cells: Fig. 5(a), cell 800, and Fig. 5(c), cell 1000, for line 1, and Fig. 5(b), cell 800, and Fig. 5(d), cell 1000, for line 2. We observe a synchronization between the waves through the two lines at the same cell [Figs. 5(a) and 5(b), then Figs. 5(c) and 5(d)]. Now, we take into account dissipation on each line ($\sigma_1 = 0.00461$ and $\sigma_2 = 0.0$). We observe in Figs. 6(a)–6(d) that the initial nonlinear excitation is well modulated. It is well known that a continuous-wave or quasicontinuous radiation propagating in a nonlinear dispersive medium may suffer instability with respect to weak periodic modulations of the steady state and results in the breaking of a continuous wave into a train of ultrashort pulses. The above input signal voltage leads to a self-modulation of the wave. It is a typical example of MI.

Figure 7 presents the behavior of waves through the line when the propagation mode is the fast mode in the absence of dissipation. Figures 7(a) and 7(c) account for cell 600, while Figs. 7(b) and 7(d) represent the propagation of waves at cell 800. As the time goes on and as the wave travels along the electrical network, we observe that the propagation seems to be chaotic on each line. The magnitude of the wave decreases exponentially. We also observe a synchronization between the waves for the two lines. But if we include through the lines the dissipation terms, the result is depicted in Fig. 8. The wave travels down the electrical network; the continuous wave breaks into a pulse train. The solitonic excitations of the pulse train have envelope functions with a familiar shape of the theory of solitonlike objects. Each element of the train has the shape of a solitonlike object. But in contrast to solitons, they emerge as a solution of the time-dependent classical equation of motion. An interesting phenomenon can be also noted in Fig. 8. The wave displays oscillating and breathing wave behavior. Indeed, it has been shown in the past that the spontaneous creation of breathers is associated with the MI of plane waves. In fact, the typical occurrence of solitonlike pulses (hereafter we called them solitons) produced by MI along the evolution of the waves is due to the interplay between the nonlinearity and dispersion. By comparison with Fig. 7, one can note that the magnitude of the waves has drastically decreased due to the presence of dissipative terms in the line. As we have seen, MI is a symmetry-breaking instability so that a small perturbation on top of a constant-amplitude background experiences exponential growth and this leads to beam breakup in either space or time. Since this disintegration typically occurs in the same parameters region where bright solitons are observed, MI is considered, to some extent, a precursor to soliton formation. MI is then responsible for the formation of envelope solitons in electrical transmission lines. MI also sets a fundamental nonlinear limiting factor in the transmission of dense wavelength-division multiplexed signals in long-distance electrical links.

Coherent structures and chaotic states are well known as two distinct states of nonlinear dissipative wave systems.

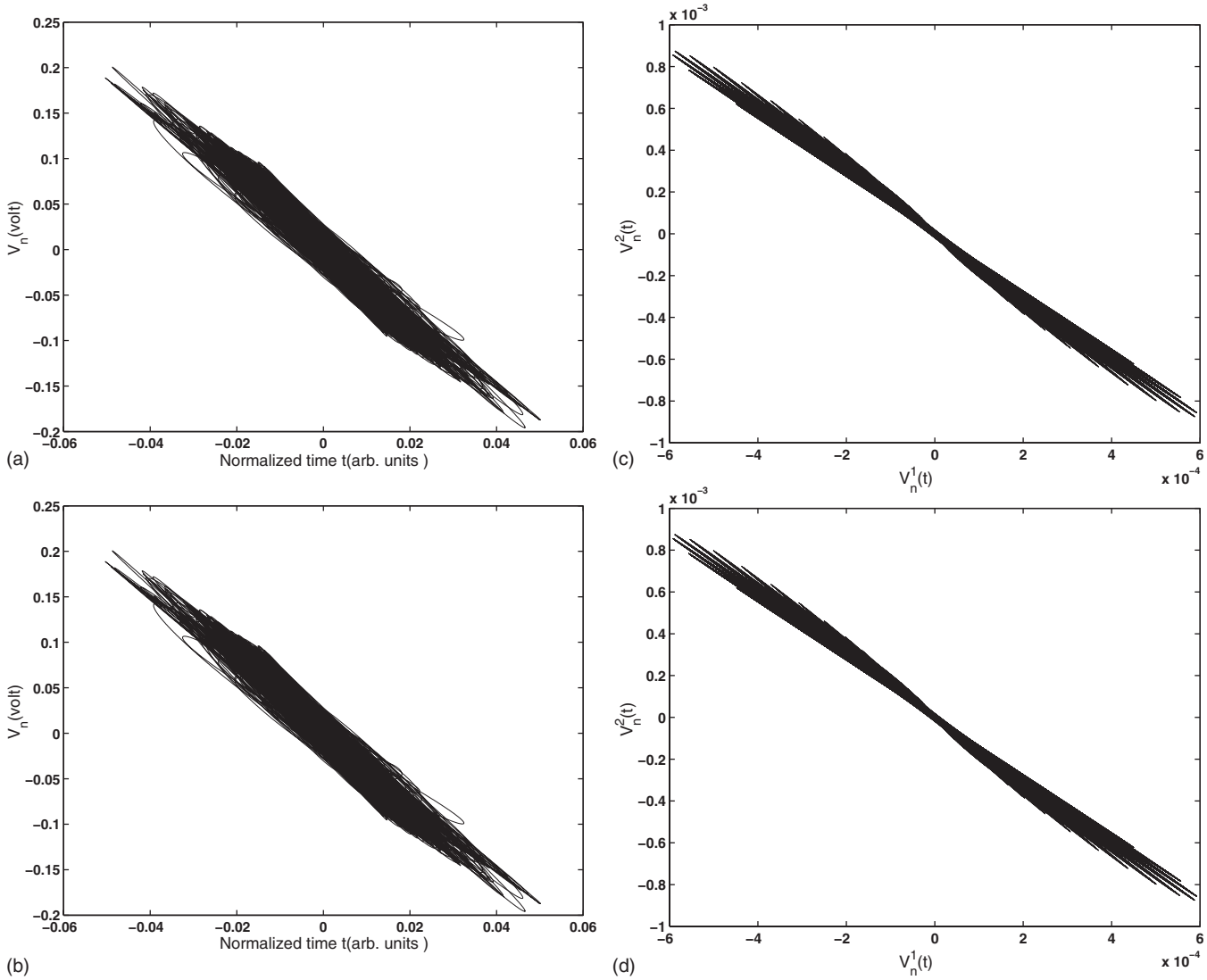

FIG. 10. Phase portrait of the fast mode at cell 800. (a) In the absence of dissipation, line 1. (b) Line 2. (c) In the presence of dissipation, cell line 2. (d) Line 2.

However, these states sometimes occur and propagate together in some systems. This incoherent evolution of modulated plane waves can be evidenced in the nonreproducibility of experiments devoted to their propagation in the nonlinear medium, as observed by Ablowitz *et al.* [34] in the context of fluid dynamics—that is, considering modulated periodic Stokes waves in deep water. For two different experiments with initial identical signals generated by the wave maker, the resulting temporal evolutions of the surface displacement at a given position in the tank are graphed against each other to produce a "phase plane" plot indicating the level of reproducibility. In particular, if the two experiments can be considered to be reproducible near the wave maker, which corresponds to a 45° line in the phase plane, on the contrary, a complex graph is obtained for more distant positions in the tank. This complex graph traduces the nonreproduciblity of both experiments and modulated periodic Stokes waves, which is attributed to the development of a phase shift between the waves of the two experiments, this unavoidable phase shift being a function of time. Here, we consider modulated plane waves in a coupled NLTL. In the phase plane plots, the evolution of the voltage is shown in Fig. 9 when the mode of propagation is the slow mode for cell 1000 [Figs. 9(a) and 9(b) in the absence of dissipation, while Figs. 9(c) and 9(d) depict the case where the dissipation is present]. Figure 10 depicts the phase plane plot when the mode of propagation is the fast mode. The graphs are obtained for cell 800 [Figs. 10(a) and 10(b) in the absence of dissipation, while Figs. 10(c) and 10(d) represent the system when dissipation is taken into account]. The geometry of the graph traduces the dynamics of nonlinear modulated waves, from pseudocoherent to a chaotic state. The chaoticlike state graph obtained here traduces the particular instability of modulated waves described through the previous figures. Furthermore, one can note that when the dissipation is present in the system, this latter seems to be less chaotic and the waves are also well decomposed into a train of pulses. One can conclude that the presence of dissipation through each line seems to reduce the chaoticlike behavior of the coupled system.

V. CONCLUSION

In this paper, we have investigated analytically and numerically MI in a coupled NLTL. We have shown that the dynamics of nonlinear waves in a coupled discrete nonlinear electrical transmission line with negative nonlinear resistance can be described by a set of coupled discrete complex Ginzburg-Landau equations. Exploiting the Stokes wave analysis, we built a typical dependence of MI gain on the perturbation wave numbers and parameters of the system. By solving the fourth-order polynomial obtained from the condition of nontrivial solutions, we show regions of MI on the (q,Q) plane. Then, outcomes of the nonlinear development of the MI predicted analytically were identified from direct simulations of the underlying CDCGL equations. This was most clearly identified for longer-time dynamical evolution results that permit one to clearly identify the instability through the formation of localized train of pulses. A stable array of stationary pulses and an apparently turbulent (chaotic) state have been obtained during the propagation. However, there are still "stronger" signatures of the instability in the unstable fast and slow modes. This work advocates the use of the MI as an experimental tool to generate solitonic trains in the NLTL. Our theoretical investigation and numerical findings clearly support the formation of such trains in the context of the NLTL. The chaoticlike state of the line has been presented. The influence of the dissipative elements on the line has also been presented.

ACKNOWLEDGMENTS

A.M. acknowledges partial support from the American Physical Society's International Travel Grant Program (ITGAP) and Dickinson College.

APPENDIX A

The coefficients of Eq. (5) are

$$d_{11} = -(\lambda_1 + 1)\omega^2 + \omega_{01}^2 + 4\mu_{01}^2 \sin^2\left(\frac{k}{2}\right),$$

$$d_{12} = -\lambda_1\omega^2, \quad d_{21} = -\lambda_2\omega^2,$$

$$d_{22} = -(\lambda_2 + 1)\omega^2 + \omega_{02}^2 + 4\mu_{02}^2 \sin^2\left(\frac{k}{2}\right). \quad \text{(A1)}$$

Coefficients of the dispersion relation (6) are

$$\lambda_j = \frac{C}{C_{0j}}, \quad 2\mu_{0j}\sigma_1 = \frac{g_{1j}}{C_{0j}}, \quad 2\mu_{0j}\sigma_2 = \frac{\alpha}{C_{0j}}, \quad a = 1 + \lambda_1 + \lambda_2,$$

$$b = (1+\lambda_1)\left[\omega_{02}^2 + 4\mu_{02}^2 \sin^2\left(\frac{k}{2}\right)\right] + (1+\lambda_2)\left[\omega_{01}^2 + 4\mu_{01}^2 \sin^2\left(\frac{k}{2}\right)\right],$$

$$c = \left[\omega_{01}^2 + 4\mu_{01}^2 \sin^2\left(\frac{k}{2}\right)\right]\left[\omega_{02}^2 + 4\mu_{02}^2 \sin^2\left(\frac{k}{2}\right)\right],$$

$$\Delta = b^2 - 4ac, \quad \omega_{0j}^2 = \frac{1}{L_{0j}C_{0j}}, \quad \mu_{0j}^2 = \frac{1}{L_jC_{0j}}. \quad \text{(A2)}$$

Coefficients of the CDCGL equation (14) are

$$Q_{jr} = \frac{3\omega^2}{(1+\lambda_j)A^2\mu_{0j}^2}, \quad Q_{ji} = \frac{4\beta\omega}{(1+\lambda_j)A\mu_{0j}^2}, \quad P_{jr} = 1,$$

$$\gamma_{jr} = -2P_{jr}, \quad \gamma_{ji} = -2P_{ji},$$

$$\Gamma_{jr} = \frac{\lambda_j\omega^2}{(1+\lambda_j)(\omega_{0j}^2 + 2\mu_{0j}^2 - (1+\lambda_j)\omega^2)},$$

$$P_{ji} = \frac{2\mu_{0j}\omega}{(1+\lambda_j)}\left[\frac{\sigma_1(\omega_{0j}^2 + 2\mu_{0j}^2 - (1+\lambda_j)\omega^2) - \mu_{0j}^2(\sigma_2 + 2\sigma_1)}{\omega_{0j}^2 + 2\mu_{0j}^2 - (1+\lambda_j)\omega^2}\right],$$

$$\Gamma_{ji} = \frac{2\lambda_j\omega^3\sigma_1}{(1+\lambda_j)\mu_{0j}[\omega_{0j}^2 + 2\mu_{0j}^2 - (1+\lambda_j)\omega^2]}. \quad \text{(A3)}$$

APPENDIX B

The elements of the matrix (22) are

$$h_{11} = -\Omega + m_1 + im_2, \quad h_{12} = m_3 + im_4,$$

$$h_{13} = -\alpha_1\Omega + m_5 + im_6,$$

$$h_{14} = 0, \quad h_{21} = m_3 - im_4, \quad h_{22} = \Omega + m_7 - im_2, \quad h_{23} = 0,$$

$$h_{24} = \alpha_1\Omega + m_8 - im_6, \quad h_{31} = -\alpha_2\Omega + m_9 + im_{10}, \quad h_{32} = 0,$$

$$h_{33} = -\Omega + m_{11} + im_{12}, \quad h_{34} = m_{13} + im_{14}, \quad h_{41} = 0,$$

$$h_{42} = \alpha_2\Omega + m_{15} - im_{10}, \quad h_{43} = m_{10} - im_{11},$$

$$h_{44} = \Omega + m_{16} - im_{12},$$

$$m_1 = \left[-4P_{1r}\cos(q)\sin^2\left(\frac{Q}{2}\right) - 2P_{1r}\sin(q)\sin(Q) + (\Gamma_{1r})\frac{\Lambda_2}{\Lambda_1} + Q_{1r}|\Lambda_1|^2\right],$$

$$m_2 = \left[-4P_{1i}\cos(q)\sin^2\left(\frac{Q}{2}\right) - 2P_{1i}\sin(q)\sin(Q) + \Gamma_{1i}\frac{\Lambda_2}{\Lambda_1} + Q_{1i}|\Lambda_1|^2\right],$$

$$m_3 = Q_{1r}|\Lambda_1|^2, \quad m_4 = Q_{1i}|\Lambda_1|^2, \quad m_5 = -\Gamma_{1r}, \quad m_6 = -\Gamma_{1i},$$

$$m_7 = \left[-4P_{1r}\cos(q)\sin^2\left(\frac{Q}{2}\right) - 2P_{1r}\sin(q)\sin(Q) + (\Gamma_{1r})\frac{\Lambda_2}{\Lambda_1} + Q_{1r}|\Lambda_1|^2\right],$$

$$m_8 = -\Gamma_{1r}, \quad m_9 = -\Gamma_{2r}, \quad m_{10} = -\Gamma_{2i},$$

$$m_{11} = \left[-4P_{2r}\cos(q)\sin^2\left(\frac{Q}{2}\right) - 2P_{2r}\sin(q)\sin(Q) + (\Gamma_{2r})\frac{\Lambda_1}{\Lambda_2} + Q_{2r}|\Lambda_2|^2 \right],$$

$$m_{12} = \left[-4P_{2i}\cos(q)\sin^2\left(\frac{Q}{2}\right) - 2P_{2i}\sin(q)\sin(Q) + \Gamma_{2i}\frac{\Lambda_1}{\Lambda_2} + Q_{2i}|\Lambda_2|^2 \right],$$

$$m_{13} = Q_{2r}|\Lambda_2|^2, \quad m_{14} = Q_{2i}|\Lambda_2|^2, \quad m_{15} = -\Gamma_{2r},$$

$$m_{16} = \left[-4P_{2r}\cos(q)\sin^2\left(\frac{Q}{2}\right) - 2P_{2r}\sin(q)\sin(Q) + (\Gamma_{2r})\frac{\Lambda_1}{\Lambda_2} + Q_{2r}|\Lambda_2|^2 \right]. \quad \text{(B1)}$$

[1] S. Flach and C. R. Willis, Phys. Rep. **295**, 181 (1998); P. G. Kevrekidis, K. O. Ransmussen, and A. R. Bishop, Int. J. Mod. Phys. B **15**, 2833 (2001).

[2] A. C. Scott and L. Macheil, Phys. Lett. **98A**, 87 (1988); A. J. Sievers, and S. Takeno, Phys. Rev. Lett. **61**, 970 (1988).

[3] W. P. Su, J. R. Schrieffer, and A. J. Heeger, Phys. Rev. Lett. **42**, 1698 (1979).

[4] A. S. Davydov, J. Theor. Biol. **38**, 559 (1973).

[5] A. Trombettoni and A. Smerzi, Phys. Rev. Lett. **86**, 2353 (2001).

[6] P. Marquie, J. M. Bilbault, and M. Remoissenet, Phys. Rev. E **49**, 828 (1994); M. Marklund and P. K. Shukla, *ibid.* **73**, 057601 (2006); K. Tse Ve Koon, J. Leon, P. Marquié, and P. Tchofo-Dinda, *ibid.* **75**, 066604 (2007).

[7] R. Stearrett and L. Q. English, J. Phys. D **40**, 5394 (2007); F. II Ndzana, A. Mohamadou, and T. C. Kofane, *ibid.* **40**, 3254 (2007); D. Yemélé, P. Marquié, and J. M. Bilbault, Phys. Rev. E **68**, 016605 (2003).

[8] A. C. Scott, *Active and Nonlinear Wave Propagation in Electronics* (Wiley-Interscience, New York, 1970).

[9] K. E. Lonngren, in *Solitons in Action*, edited by K. E. Lonngren and A. C. Scott (Academic, New York, 1978).

[10] R. Hirota and K. Suzuki, J. Phys. Soc. Jpn. **28**, 1366 (1970); Proc. IEEE **61**, 1483 (1973).

[11] H. Nagashima and Y. Amagishi, J. Phys. Soc. Jpn. **45**, 860 (1978).

[12] M. Toda, J. Phys. Soc. Jpn. **23**, 501 (1967).

[13] E. Kengne and W. M. Liu, Phys. Rev. E **73**, 026603 (2006); F. B. Pelap and M. M. Faye, J. Math. Phys. **46**, 033502 (2005).

[14] P. Marquié, J. M. Bilbault, and M. Remoissenet, Phys. Rev. E **51**, 6127 (1995); M. Remoissenet, *Waves Called Solitons*, 3rd ed. (Springer, Berlin, 1999).

[15] F. B. Pelap, T. C. Kofane, N. Flytzanis, and M. Remoissenet, J. Phys. Soc. Jpn. **70**, 2568 (2001).

[16] J. M. Bilbault, P. Marquié, and B. Michaux, Phys. Rev. E **51**, 817 (1995); E. Kengne, S. T. Chui, and W. M. Liu, *ibid.* **74**, 036614 (2006).

[17] T. Kakutani and N. Yamasaki, J. Phys. Soc. Jpn. **45**, 674 (1978); T. Yoshinaga and T. Kakutani, *ibid.* **49**, 2072 (1980).

[18] B. Z. Essimbi, A. M. Dikande, T. C. Kofane, and A. A. Zibi, J. Phys. Soc. Jpn. **64**, 2361 (1995); B. Z. Essimbi, L. Ambassa, and T. C. Kofane, Physica D **106**, 207 (1997); D. Yemele and T. C. Kofane, J. Phys. D **39**, 4504 (2006).

[19] T. Taniuti and N. Yajima, J. Math. Phys. **10**, 1369 (1969).

[20] J. F. Ravoux, S. Le Dizes, and P. Le Gal, Phys. Rev. E **61**, 390 (2000); T. Yokoi, H. Yamada, and K. Nozaki, J. Phys. Soc. Jpn. **73**, 358 (2004); A. Mohamadou, A. K. Jiotsa, and T. C. Kofané, Phys. Rev. E **72**, 036220 (2005).

[21] P. Marquié, S. Binczak, J. C. Comte, B. Michaux, and J. M. Bilbault, Phys. Rev. E **57**, 6075 (1998).

[22] J. S. Comte, P. Marquie, J. M. Bilbault, and S. Binczak, Ann. Telecommun. **53**, 483 (1998).

[23] H. K. Nguena, S. Noubissi, and P. Woafo, J. Phys. Soc. Jpn. **73**, 1147 (2004).

[24] A. C. Newell and J. A. Whitehead, in *Proceedings of the International Union of Theoretical and Applied Mechanics Symposium on Instability of Continuous Systems, Herrenalb, Germany, 1969*, edited by H. Leipholz (Springer, Berlin, 1971), p. 279.

[25] K. Stewartson and J. T. Stuart, J. Fluid Mech. **48**, 529 (1971).

[26] R. C. DiPrima, W. Eckhaus, and L. A. Segal, J. Fluid Mech. **49**, 705 (1971).

[27] M. C. Cross and P. C. Hohenberg, Rev. Mod. Phys. **65**, 851 (1993); I. S. Aranson and L. Kramer, *ibid.* **74**, 99 (2002); H. Willaime, O. Cardoso, and P. Tabeling, Phys. Rev. Lett. **67**, 3247 (1991).

[28] S. S. Wang and H. G. Winful, Appl. Phys. Lett. **52**, 1774 (1988); N. K. Efremidis and D. N. Christodoulides, Phys. Rev. E **67**, 026606 (2003).

[29] K. Porsezian, R. Murali, B. A. Malomed, and R. Ganapathy, Chaos, Solitons Fractals **9**, 86 (2007).

[30] B. Tan and S. Liu, J. Atmos. Sci. **52**, 1501 (1995).

[31] P. Marquie and J. M. Bilbault, Phys. Lett. A **174**, 250 (1993).

[32] D. C. Hutchings and J. M. Arnold, J. Opt. Soc. Am. B **16**, 513 (1999).

[33] R. Lai and A. J. Sievers, Phys. Rev. B **57**, 3433 (1998).

[34] M. J. Ablowitz, J. Hammack, D. Henderson, and C. M. Schober, Physica D **152-153**, 416 (2001).